Supporting information

Tripyridinophane Platform Containing Three Acetate Pendant Arms: An Attractive Structural Entry for the Development of Neutral Eu(III) and Tb(III) Complexes in Aqueous Solution.

Nadine Leygue,[†] Chantal Galaup,[†] Alberto Lopera,[‡] Estefanía Delgado-Pinar,[‡] René M. Williams,[⊥] Heinz Gornitzka,[§] Jurriaan M. Zwier,[≠] Enrique García-España,[‡] Laurent Lamarque,[*,≠] Claude Picard[*,†]

[†] Laboratoire de Synthèse et Physico-Chimie de Molécules d'Intérêt Biologique (SPCMIB), Université Paul Sabatier-Toulouse III/ CNRS (UMR5068), 118 route de Narbonne, F-31062 Toulouse, France

[‡] Instituto de Ciencia Molecular (ICMOL), Universitat de València, C/ Catedrático José Beltrán 2, 46980 Paterna, Spain

[⊥] Molecular Photonics Group, Van 't Hoff Institute for Molecular Sciences, University of Amsterdam, P.O. Box 94157, 1090 GD Amsterdam, The Netherlands

[§] CNRS, LCC, Université de Toulouse, UPS, INPT, 205 Route de Narbonne, F-31077 Toulouse Cedex 4, France

[≠] Cisbio bioassays, Parc Marcel Boiteux, BP 84175, 30200 Codolet, France.

Corresponding Authors

* E-mail for C.P.: picard@chimie.ups-tlse.fr

* E-mail for L.L.: llamarque@cisbio.com

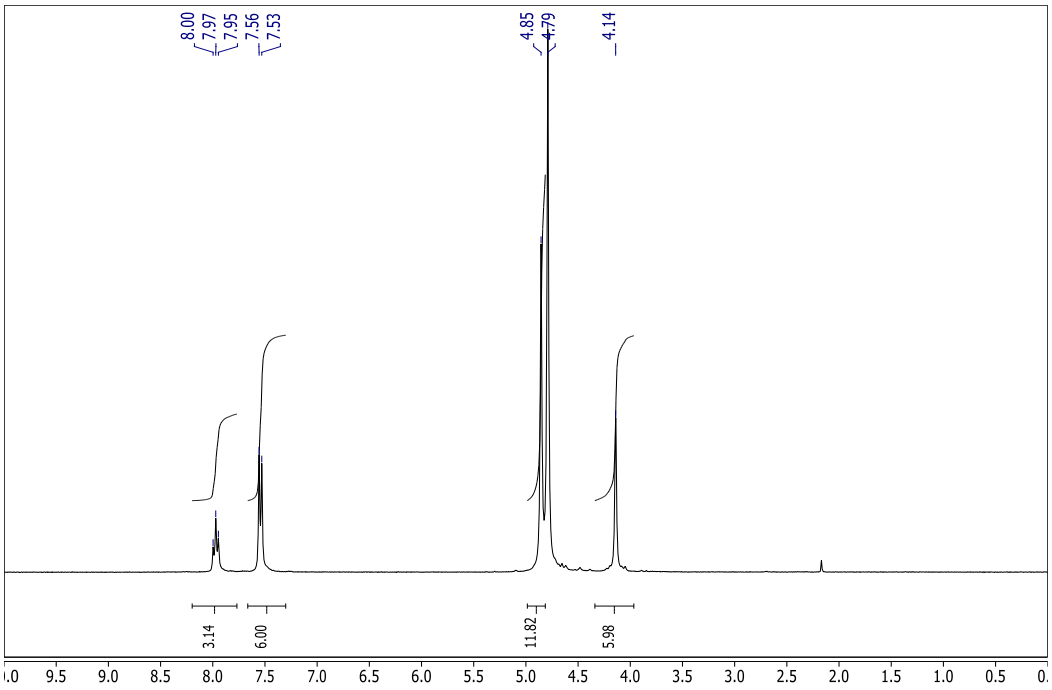

Figure S1: ^{1}H NMR (300MHz, D_2O) spectrum of H_3tpptac ligand.

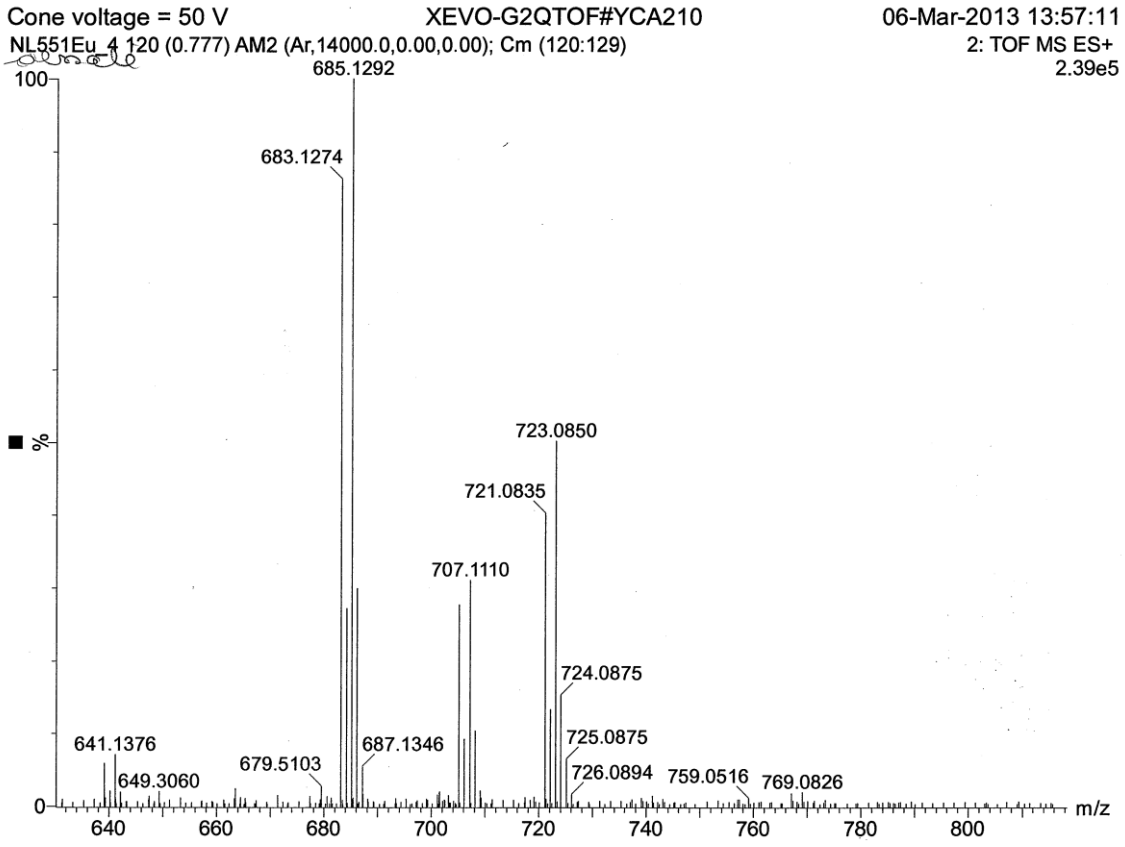

Figure S2: MS (ESI+) spectrum of Eutpptac complex

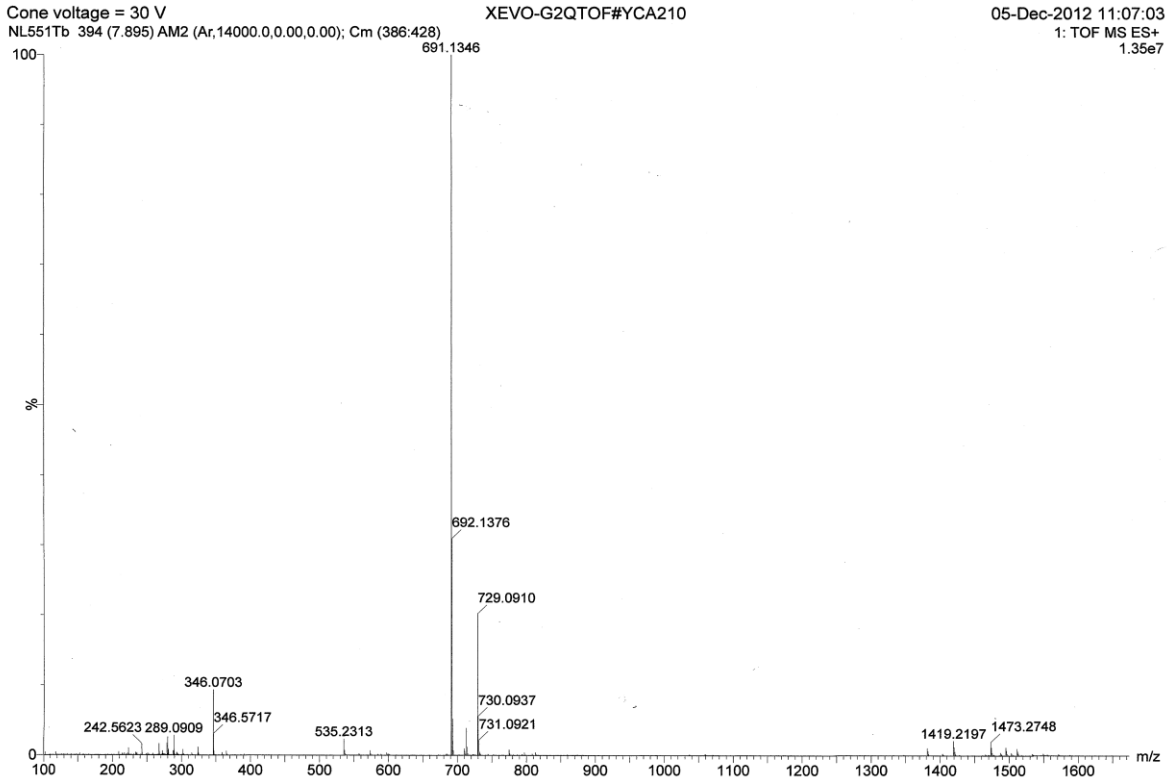

Figure S3: MS (ESI+) spectrum of Tbtpptac complex

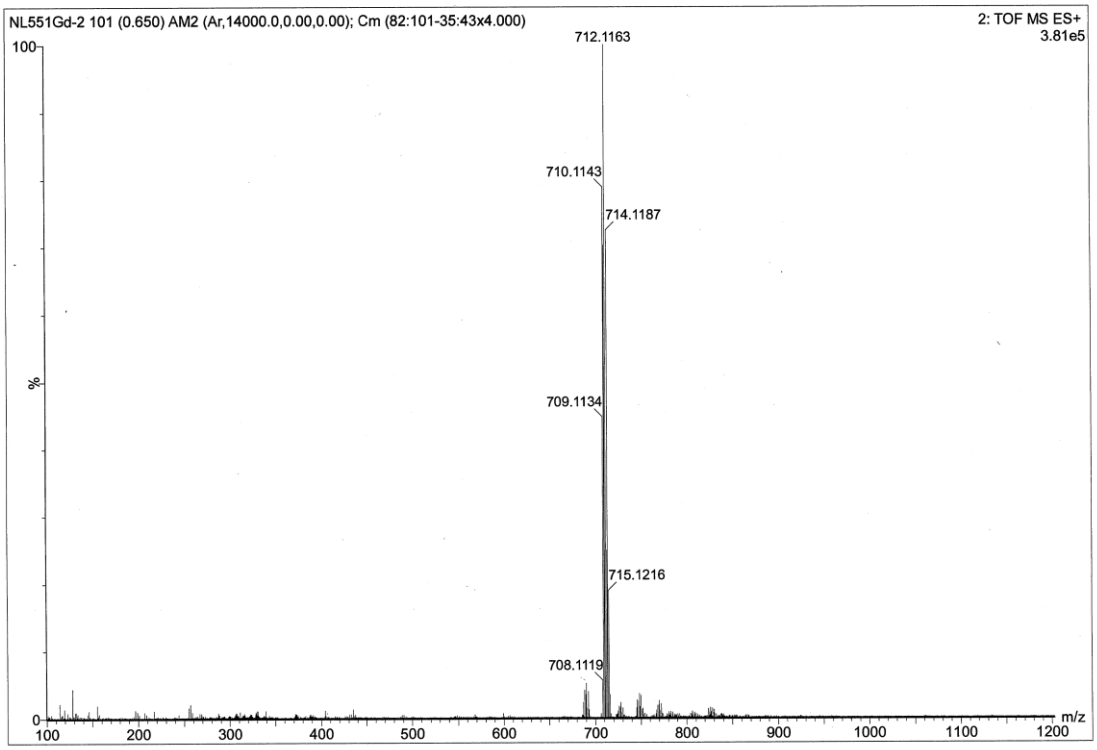

Figure S4: MS (ESI+) spectrum of Gdtpptac complex

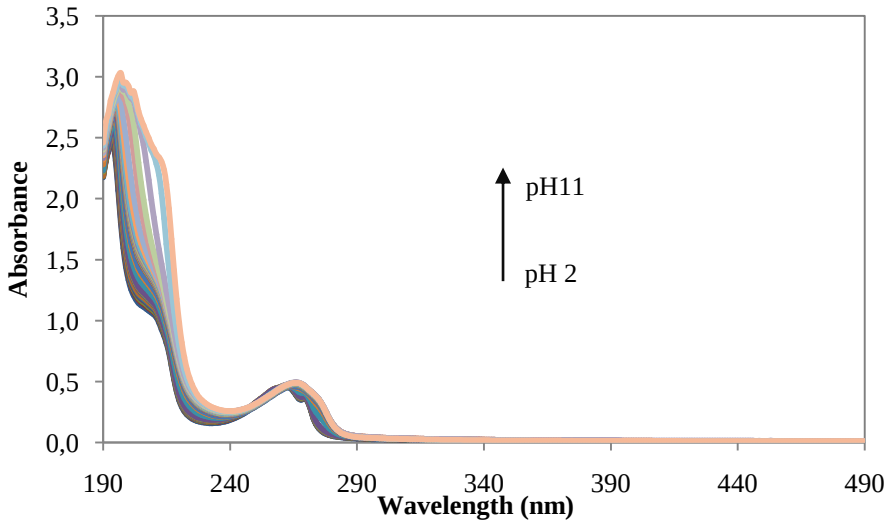

Figure S5. UV–Vis spectrum for the H_3tpptac ligand at different pH values. [ligand] = $5x10^{-5}$M.

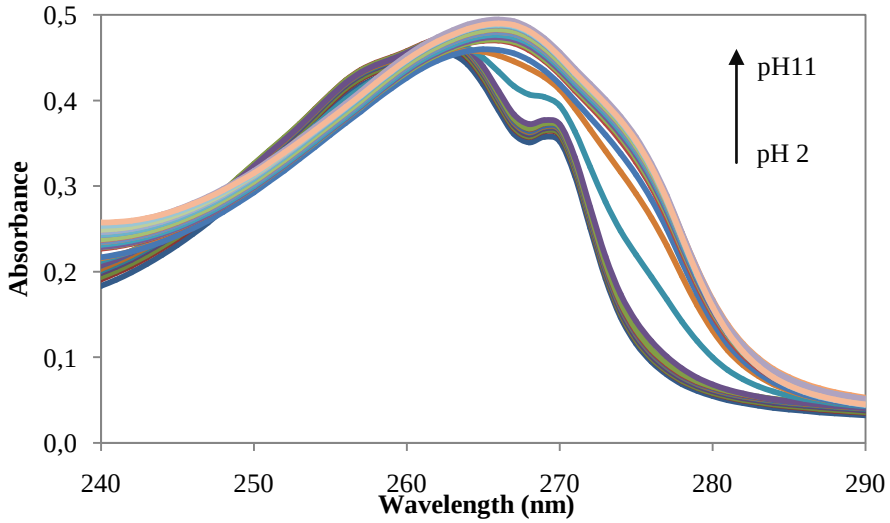

Figure S6. UV–Vis spectrum for the H_3tpptac ligand at different pH values from 240 to 290 nm. [Ligand] = $5x10^{-5}$M.

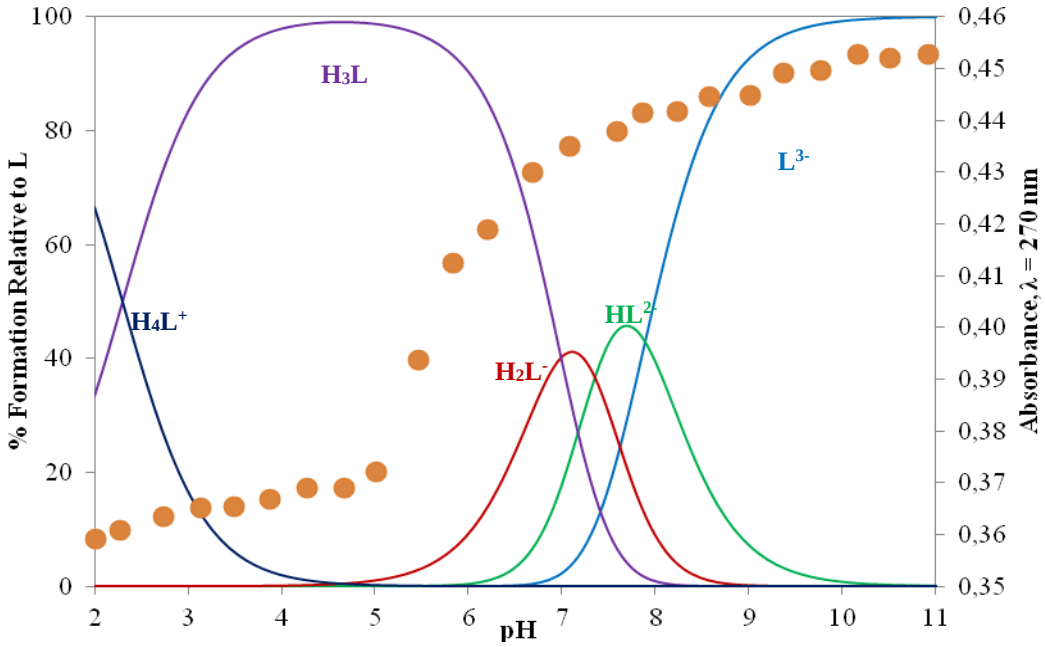

Figure S7. Plot of the species distribution diagram for H_3tpptac ligand along with the variations with pH of the absorbance at 270 nm. [Ligand$^-$] = 5x10^{-5}M. pH values: 2.01, 2.28, 2.74, 3.13, 3.49, 3.88, 4.28, 4.67, 5.01, 5.47, 5.84, 6.21, 6.69, 7.09, 7.60, 7.87, 8.24, 8.58, 9.01, 9.37, 9.77, 10.17, 10.51 and 10.92.

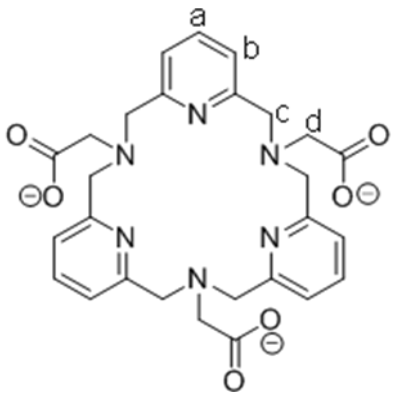

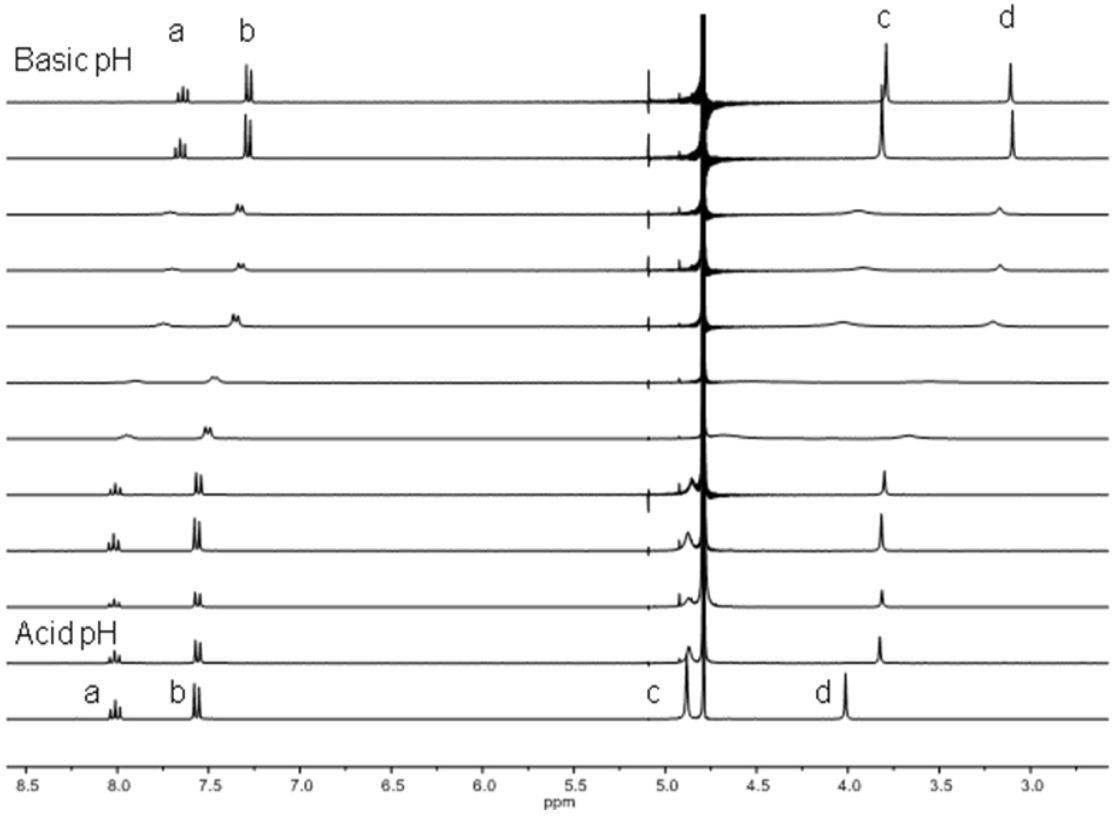

Figure S8. ^{1}H NMR spectra for H_3tpptac ligand at different pH values, from the bottom to the top: 1.45, 3.05, 4.03, 4.71, 6.02, 7.19, 7.52, 8.11, 8.55, 8.96, 10.23 and 11.69.

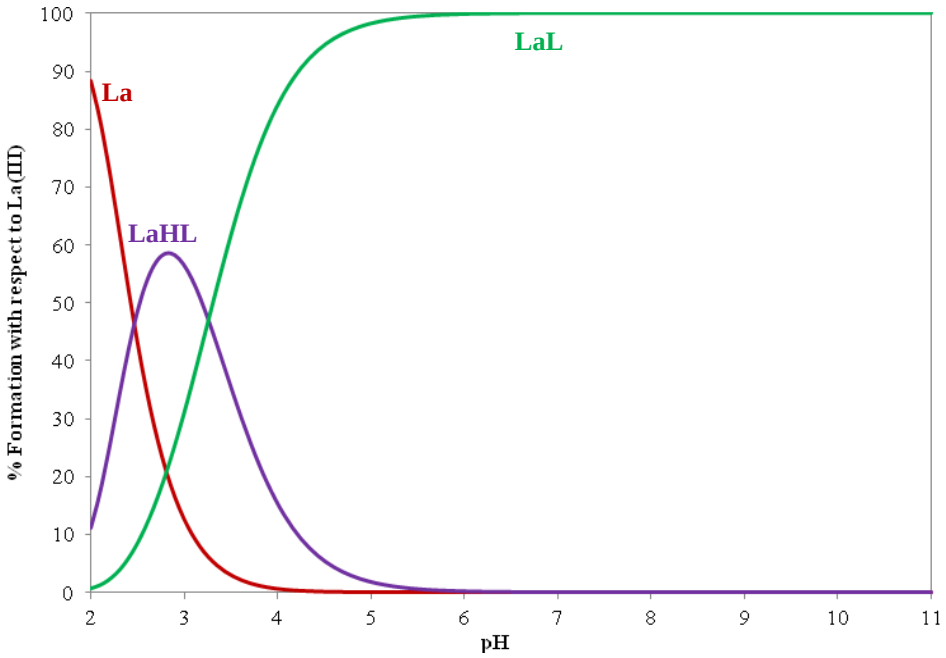

Figure S9**.** Distribution diagram for the system H_3tpptac-La(III) as a function of the pH. [Ligand] = [La(III)] = 10^{-3}M.

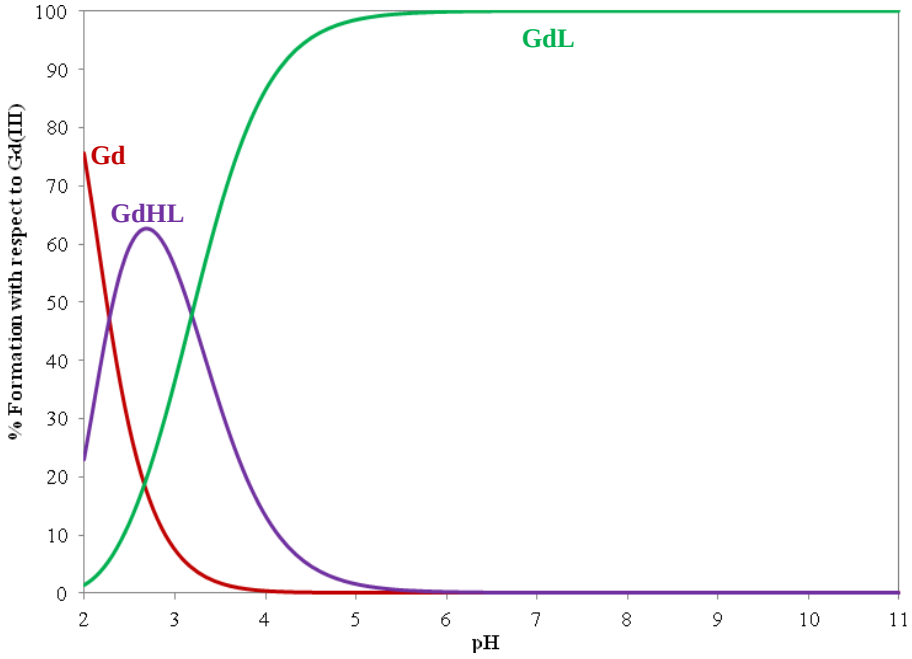

Figure S10**.** Distribution diagram for the system H_3tpptac-Gd(III) as a function of the pH. [Ligand] = [Gd(III)] = 10^{-3}M.

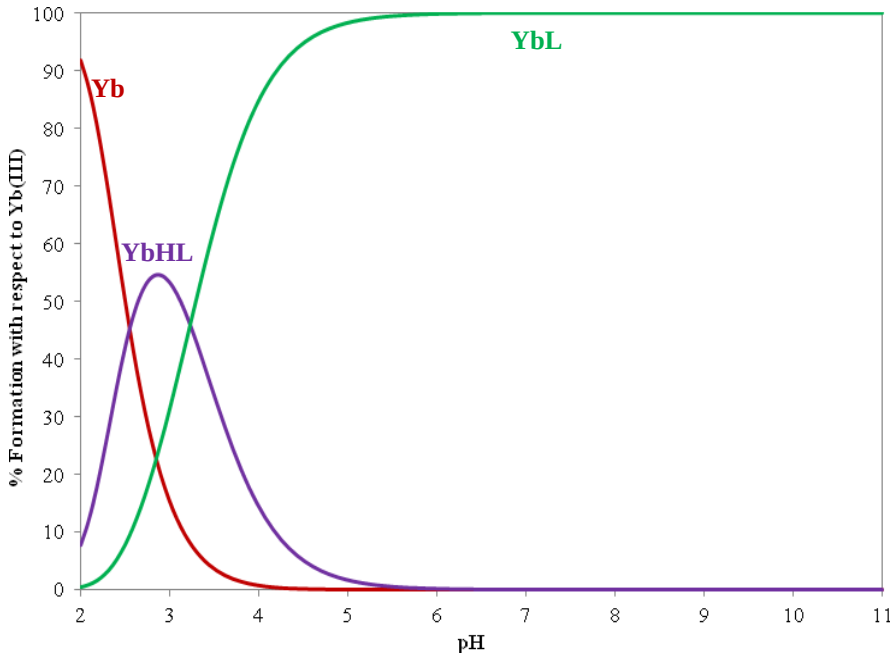

Figure S11. Distribution diagram for the system H_3tpptac-Yb(III) as a function of the pH. [Ligand] = [Yb(III)] = 10^{-3}M.

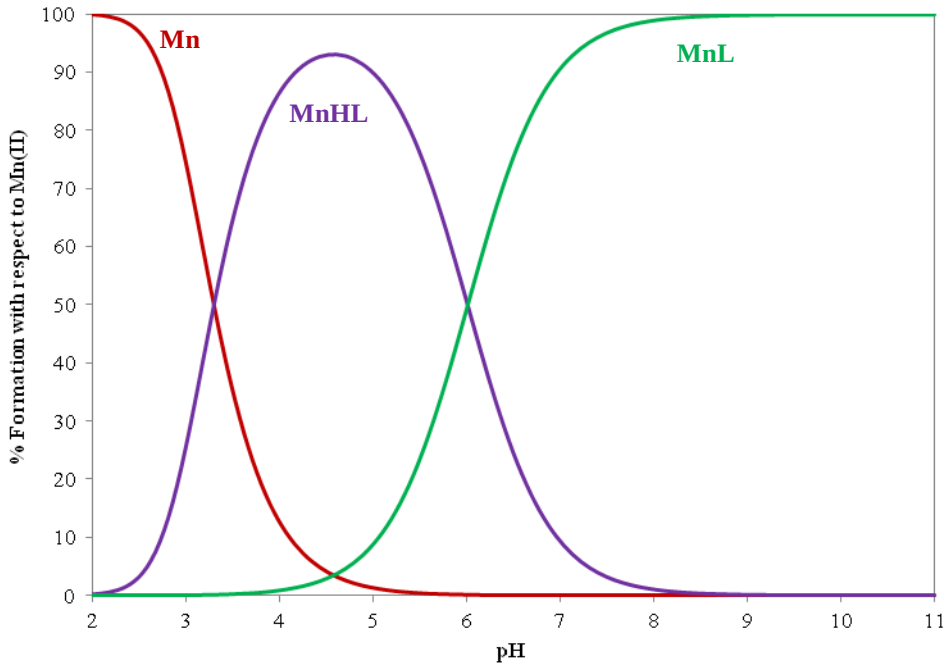

Figure S12. Distribution diagram for the system H_3tpptac-Mn(II) as a function of the pH. [Ligand] = [Mn(II)] = 10^{-3}M.

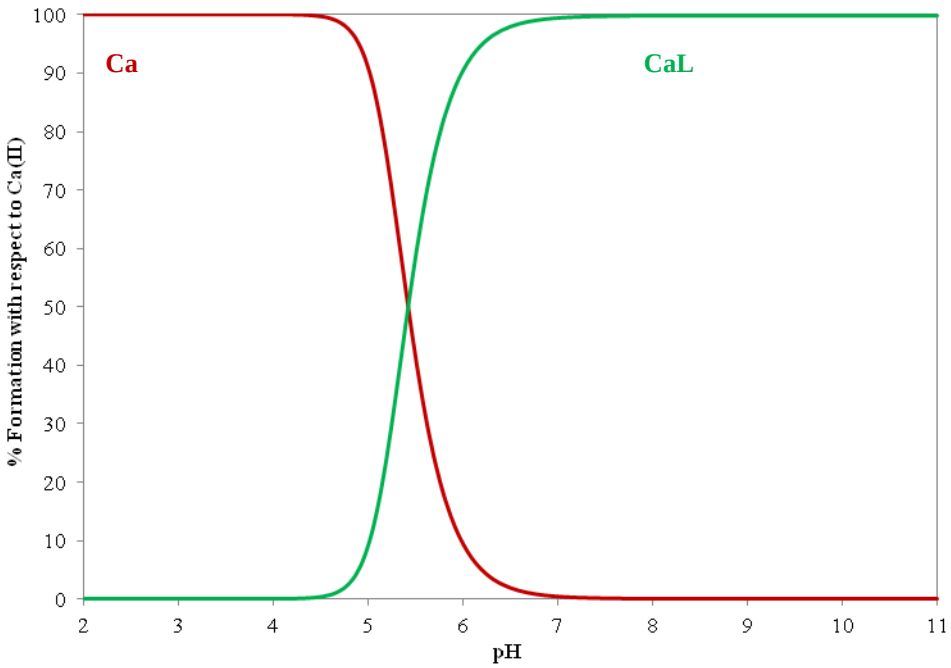

Figure S13**.** Distribution diagram for the system H_3tpptac-Ca(II) as a function of the pH. [Ligand] = [Ca(II)] = 10^{-3}M.

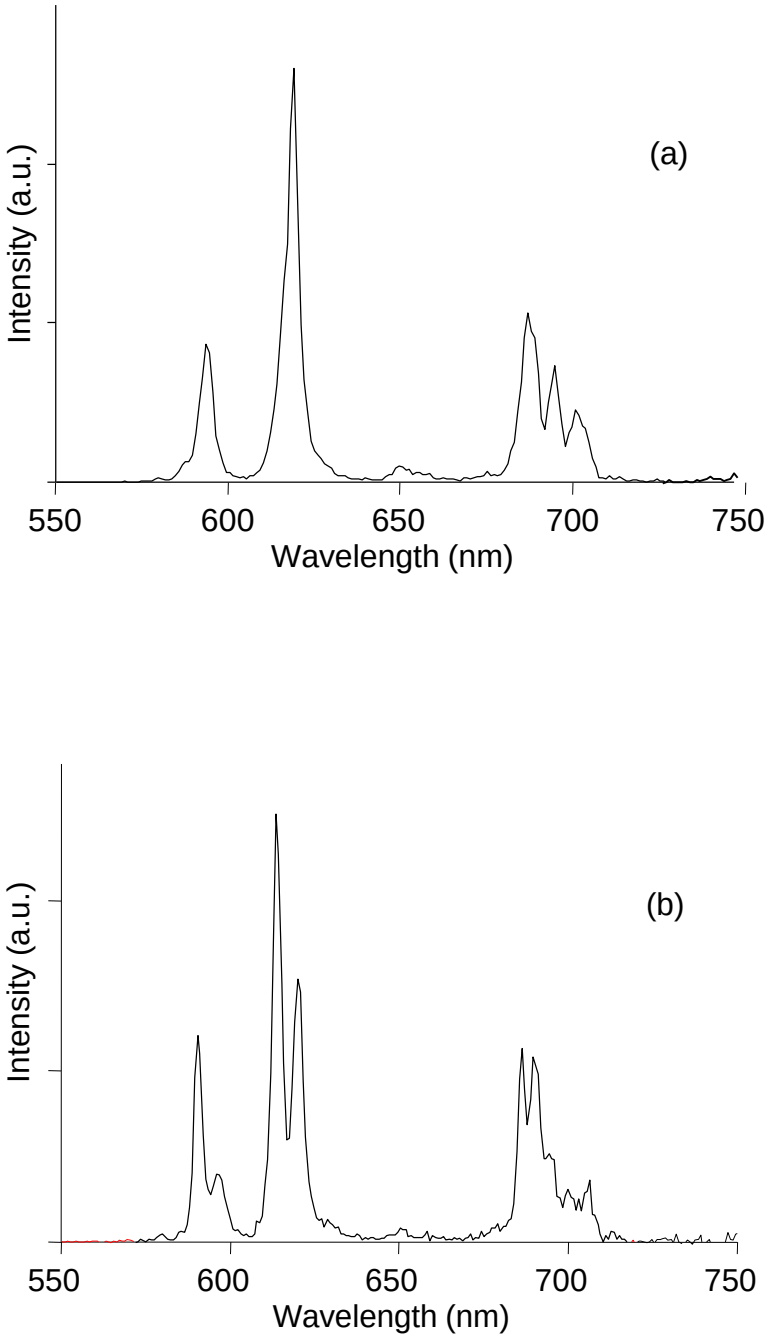

Figure S14. Low resolution corrected emission spectra of Eutpptac in Tris buffer (pH 7.4) at 298 K without (a) and in the presence of 0.4 M KF (b). λ_{exc} = 267 nm, excitation and emission band passes 5 and 2.5 nm, respectively.

Table S1. Crystallographic for the [Tbtpptac(H_2O)] structure

Empirical formula	C27 H27 N6 O17.50 Tb	
Formula weight	874.46	
Temperature	100(2) K	
Wavelength	0.71073 Å	
Crystal system	Triclinic	
Space group	P-1	
Unit cell dimensions	a = 12.2405(8) Å	α= 90.694(2)°.
	b = 12.4167(9) Å	β= 107.946(2)°.
	c = 12.6164(9) Å	γ = 93.240(2)°.
Volume	1820.4(2) $Å^3$	
Z	2	
Density (calculated)	1.595 Mg/m^3	
Absorption coefficient	2.023 mm^{-1}	
F(000)	872	
Crystal size	0.300 x 0.300 x 0.200 mm^3	
Theta range for data collection	5.098 to 28.282°.	
Index ranges	-16<=h<=16, -16<=k<=16, -16<=l<=16	
Reflections collected	58284	
Independent reflections	8988 [R(int) = 0.0542]	
Completeness to theta = 25.242°	99.1 %	
Absorption correction	Semi-empirical from equivalents	
Max. and min. transmission	0.7461 and 0.6220	
Refinement method	Full-matrix least-squares on F^2	
Data / restraints / parameters	8988 / 138 / 577	
Goodness-of-fit on F^2	1.098	
Final R indices [I>2sigma(I)]	R1 = 0.0553, wR2 = 0.1408	
R indices (all data)	R1 = 0.0707, wR2 = 0.1600	
Extinction coefficient	n/a	
Largest diff. peak and hole	3.005 and -1.991 e.$Å^{-3}$	

Table S2. Selected angles (deg) for the [Tbtpptac(H_2O)] structure

O(3)-Tb(1)-O(1)	73.78(15)	O(5)-Tb(1)-N(2)	78.19(17)
O(3)-Tb(1)-O(5)	74.39(15)	O(7)-Tb(1)-N(2)	86.17(16)
O(1)-Tb(1)-O(5)	74.58(17)	N(1)-Tb(1)-N(2)	62.52(17)
O(3)-Tb(1)-O(7)	136.50(15)	N(3)-Tb(1)-N(2)	59.92(15)
O(1)-Tb(1)-O(7)	135.63(15)	N(5)-Tb(1)-N(2)	154.44(17)
O(5)-Tb(1)-O(7)	135.32(15)	O(3)-Tb(1)-N(6)	77.88(16)
O(3)-Tb(1)-N(1)	131.43(14)	O(1)-Tb(1)-N(6)	136.88(16)
O(1)-Tb(1)-N(1)	120.98(16)	O(5)-Tb(1)-N(6)	66.84(18)
O(5)-Tb(1)-N(1)	67.55(16)	O(7)-Tb(1)-N(6)	86.85(15)
O(7)-Tb(1)-N(1)	68.08(15)	N(1)-Tb(1)-N(6)	60.21(17)
O(3)-Tb(1)-N(3)	120.14(15)	N(3)-Tb(1)-N(6)	155.03(16)
O(1)-Tb(1)-N(3)	67.88(15)	N(5)-Tb(1)-N(6)	61.56(18)
O(5)-Tb(1)-N(3)	131.77(16)	N(2)-Tb(1)-N(6)	120.55(17)
O(7)-Tb(1)-N(3)	68.19(14)	O(3)-Tb(1)-N(4)	66.80(15)
N(1)-Tb(1)-N(3)	107.68(15)	O(1)-Tb(1)-N(4)	78.45(15)
O(3)-Tb(1)-N(5)	68.59(15)	O(5)-Tb(1)-N(4)	137.48(16)
O(1)-Tb(1)-N(5)	131.57(16)	O(7)-Tb(1)-N(4)	86.45(15)
O(5)-Tb(1)-N(5)	120.88(17)	N(1)-Tb(1)-N(4)	154.46(17)
O(7)-Tb(1)-N(5)	68.31(15)	N(3)-Tb(1)-N(4)	61.85(14)
N(1)-Tb(1)-N(5)	106.75(17)	N(5)-Tb(1)-N(4)	59.43(16)
N(3)-Tb(1)-N(5)	106.67(15)	N(2)-Tb(1)-N(4)	119.68(15)
O(3)-Tb(1)-N(2)	136.51(16)	N(6)-Tb(1)-N(4)	118.66(17)
O(1)-Tb(1)-N(2)	66.72(16)		

Table S3. Logarithms of the stability constants of H_3tpptac and different chelators with Gd^{3+}, Cu^{2+}, Zn^{2+} ions.

Ligand	H_3tpptac	H_3pcta[a]	H_4Pyta[b]	N-ac$_3$ [18] aneN$_3$O$_3$[c]	H_4dota[d]	H_5dtpa[e]	H_3tpatcn[f]
logK_{Gd}	18.1	20.4	21.7	18.0	24.7	22.4	17.4
logK_{Cu}	14.4	18.8	18.6	14.9	24.8	21.2	16.2
logK_{Zn}	12.9	20.5	18.1	9.9	20.2	18.2	16.0

[a] from Tircso, G.; Kovacs, Z.; Sherry, A. D. Equilibrium and Formation/Dissociation Kinetics of Some Ln^{III}PCTA Complexes. *Inorg. Chem.* **2006**, *45*, 9269-9280.
[b] from Miao, L.; Bell, D.; Rothremel JR, G. L.; Bryant JR, L. H.; Fitzsimmons, P. M.; Jackels, S. C. Design and synthesis of an "ultrachelating" ligand based on an 18-membered ring hexaaza macrocycle. *Supramol. Chem.* **1996**, *6*, 365-373.
[c] from Delgado, R.; Sun, Y.; Motekaitis, R. J.; Martell, A. E. Stabilities of divalent and trivalent metal ion complexes of macrocyclic triazatriacetic acids. *Inorg. Chem.* **1993**, *32*, 3320-3326.
[d] from Gündüz, S.; Vibhute, S.; Botar, R.; Kalman, F. K.; Toth, I.; Tircso, G.; Regueiro-Figueroa, M.; Esteban-Gomez, D.; Platas-Iglesias, C.; Angelovski, G. Coordination Properties of GdDO3A-Based Model Compounds of Bioresponsive MRI Contrast Agents. *Inorg. Chem.* **2018**, *57*, 5973-5986.
[e] from Bonnet, C. S.; Buron, F.; Caillé, F.; Shade, C. M.; Drahos, B.; Pellegatti, L.; Zhang, J.; Villette, S.; Helm, L.; Pichon, C.; Suzenet, F.; Petoud, S.; Toth, E. Pyridine-based lanthanide complexes combining MRI and NIR luminescence activities. *Chem. Eur. J.* **2012**, *18*, 1419-1431.
[f] from Nocton, G.; Nonat, A.; Gateau, C.; Mazzanti, M. Water Stability and Luminescence of Lanthanide Complexes of Tripodal Ligands Derived from 1,4,7-Triazacyclononane: Pyridinecarboxamide versus Pyridinecarboxylate Donors. *Helv. Chim. Acta* **2009**, *92*, 2257-2273.